Expansion Strategies for Power Distribution Systems: Including Distributed Generation and Electric Vehicle

Siavash Darbani[1], Mojtaba Beiraghi[1,*], and Reza Ghanizadeh[1]

[1] *Department of Electrical Engineering, Ur.C., Islamic Azad University, Urmia, Iran*
**Corresponding author: mojtaba.beiraghi@iau.ac.ir*

Manuscript received 11 May, 2025; revised 26 November, 2025; accepted 17 December, 2025. Paper no. JEMT-2505-1552.

The increasing adoption of electric vehicles has introduced a new electric load on the grid, which differs from the traditional load profiles found in networks. Additionally, renewable energy sources significantly influence the generation patterns in these networks due to their inherent uncertainty and large fluctuations in generation. This paper introduces a multi-objective distribution system expansion model that takes into account investments in new equipment, including renewable energy sources, energy storage, and electric vehicle charging stations. The required charging for electric vehicles is determined based on their travel patterns throughout the day, considering each charge. Uncertainty in both the load and renewable resources is addressed by generating possible scenarios derived from their probability distribution curves. The final stochastic model aims to minimize the expected expansion costs of the system, including the present value of investments, maintenance, generation costs, losses, and unmet demand. The deterministic equivalent model, which incorporates a random-axis scenario model, is an integer optimization problem solved using a genetic algorithm. Numerical simulations were conducted on a 9-bus network as a small example, followed by analysis on the standard 30-bus network. The results indicate that the implementation of distributed generation sources improves losses and voltage conditions, often leading to a preference for developing distributed generation rather than expanding substations. The findings suggest that the growth of distributed generation has resulted in significant delays in substation expansion, offering an alternative that can achieve much better technical outcomes in place of substation expansion.

Keywords: *Expansion Planning, Distribution Network, Storage, Electric vehicles, Renewable Resources.*

http://dx.doi.org/10.22109/jemt.2025.522704.1552

Nomenclature

a	Equipment index
b	Time block index (day/night)
ch	Charging station index for electric vehicles
I, j	Node indices
k	Investment option index
l	Feeder type index
p	Distributed generation (DG) type index
q	Time step index
t, τ	Planning stage indices
tr	Transformer index
ω	Scenario index
Sets	
A	Set of equipment
B	Set of time blocks
CH	Set of electric vehicle parking types
L	Set of feeder types
$K^l.K^{tr}.K^p.K^{ST}.K^{ch}$	Set of available options for feeders, transformers, DG units, substations, and parking facilities
P	Set of DG types
Q	Set of yearly periods
T	Set of time stages in planning
TR	Set of transformer types
Ω^N	Set of system nodes
Ω_i^l	Nodes connected to node i via feeder type l
Ω_t^{LN}	Load nodes
Ω^{SS}	Substation nodes
Ω^p	Candidate nodes for DG
Ω^{ST}	Candidate nodes for storage
Ω^{ch}	Candidate nodes for EV charging parking
$\prod$	Set of scenarios
γ^l	Set of branches with feeder type l

Parameters

$C_k^{I.l}$	Investment costs for feeders
$C_i^{I.SS}$	Substations
$C_k^{I.NT}$	Transformers
$C_k^{I.p}$	DG units
$C_k^{I.ST}$	Storage systems
$C_k^{I.ch}$:	Charging parking stations
$C_k^{M.l}$	Maintenance costs for feeders
$C_k^{M.tr}$	Transformers
C_k^{M}	DG units
$C_k^{M.ST}$	Storage systems
$C_k^{M.ch}$	Charging parking stations
$C_{tqb\omega}^{SS}$	Cost of power supply from substations
$C_k^{E.p}$	Cost of DG production
$C_k^{ST.prod}$	Cost of storage system production
$C_k^{ST.store}$	Cost of energy storage in storage systems
$D_{itqb\omega}$	Load on the system
$d_{\text{dem}}^{tqb\omega}$	Total demand for charging electric vehicles in the system
$\bar{F}_{ijk}^{lV}$	Theoretical power capacity of feeders
$\bar{G}_k^{tr}$	Theoretical power capacity required for supply through transformers
$\bar{G}_k^{p}$	Power generation capacity of generator type p
$\hat{G}_{iktqb\omega}^{p}$	Power availability from generator type p
$\underline{G}_k^{ST}$	Minimum capacity of storage units
$\bar{G}_k^{ST}$	Maximum capacity of storage units
$\bar{G}_k^{ch}$	Parking capacity
I	Annual investment rate
IB_t	Investment limit at stage t
l_{ij}	Length of feeders
$n_{DG}.n_T$	Number of candidate groups for DG and the number of scheduling stages
pf	Power factor of the system
RR^a	Rate of return on investment per equipment
$Z_k^l.Z_k^{tr}$	Feed capacity of unit type l and transformer capacity
$\pi_{qb\omega}$	Weight of scenario
Δ_{qb}	Duration of each time block
$\eta_{ik}^{ST.prod}$	Efficiency of power generation by storage units
$\eta_{ik}^{ST.store}$	Efficiency of energy storage by storage units
ε	Limitations on power source penetration
v^a	Lifetime of each equipment
c_t^I	Cost of Investment at Stage t
c_t^E	Cost of Power Production at Stage t
c_t^M	Cost of Maintenance at Stage t
c_t^R	Cost of Power Loss at Stage t
c_t^U	Cost of Unmet Power Demand at Stage t
$d_{itqb\omega}^{ch}$	Electric Vehicle Charging Demand in Group i
$d_{itqb\omega}^{U}$	Unmet Power Demand for Each Group
$f_{ijktqb\omega}^{l}$	Power Flow Through the Feeder
$g_{iktqb\omega}^{p}$	Energy Supplied by Generator Type p
$g_{iktqb\omega}^{tr}$	Energy Supplied by Transformer Type tr
$g_{iktqb\omega}^{ST.prod}$	Power Generation Capability of Storage System
$g_{iktqb\omega}^{ST.store}$	Power Stored in the Storage System
x_{it}^{SS}	Binary Variable for Investment in Pasts
x_{ikt}^{NT}	Transformers
x_{ijkt}^{l}	Feeders
x_{ikt}^{p}	DG
x_{ikt}^{ST}	Storage Systems
x_{ikt}^{ch}	Charging Parking
$u_{iktqb\omega}^{ST.prod}.u_{iktqb\omega}^{ST.store}$	Binary Variable for Storage System or Energy Storage Capacity Provision
$y_{ijkt}^{l}.y_{ikt}^{p}.y_{ikt}^{ST}.y_{ikt}^{ch}$	Binary Variable for the Use of Past, Transformer, Feeder, DG, Storage System, and Charging Parking
$v_{itqb\omega}$	Voltage of Node

Variables for Electric Vehicles

$\mathcal{H}\{1 \dots H\}$	Set of Residential Homes
$\mathcal{K} \subset \mathcal{H}$	Set of Electric Vehicles in Each Home
$\mathcal{T}\{1 \dots T\}$	Set of Discrete Time Intervals in the Charging Horizon
$\chi_{k.t}$	The current (A) drawn by the k -th vehicle at time t.
$x_{h.t}$	The current (A) drawn by the h -th household at time t.
$x_{h.t}^{\text{tot}}$	Total current (A) drawn by household h th (including both household and vehicle load)
$x_{\phi.t}$	Total current (A) drawn by all single-phase loads from phase $\phi \in \{A.B.C\}$
$s_k(t)$	Stored energy (kWh) in vehicle k -th at time t.
$s^{\max}$	Maximum allowable stored energy (kWh).
τ	Charging efficiency factor.
$V_{T.x}$	Phase- to- neutral voltage of the source (V) at the transformer.
$P_{Tx}^{\max}$	Rated power of the distribution transformer (kVA)

$x_{\phi}^{\max}$	Maximum current (A) in phase $\phi \in \{A.B.C\}$,for the main feeder cable.
$x_{k}^{\max}$	Maximum current (A) in the service line connecting household k - th to the feeder.
$V_{h.t}^{\text{drop}}$	Phase- to- neutral voltage difference between the transformer and the source voltage (V).

1. Introduction

Expansion strategies for power distribution systems are crucial for accommodating increasing demand and integrating emerging technologies such as distributed generation (DG), electric vehicles (EVs), and energy storage systems. Recent studies have highlighted the importance of planning and optimizing the growth of distribution networks to improve their efficiency, reliability, and sustainability under various uncertainties. A significant focus in the expansion of distribution systems is the incorporation of renewable energy sources and distributed generation. Borges and Martins [4] explore multistage expansion planning for active distribution networks, considering uncertainties in demand and DG. Their research highlights the need for flexibility in distribution network planning to accommodate both load growth and distributed generation, ensuring the network can handle variable generation and avoid overloads. Similarly, Muñoz-Delgado et al. [6] discuss the integration of generation and network expansion planning, emphasizing the importance of considering uncertainties such as renewable energy variability and system reliability in their planning models. Another key factor in power distribution system expansion is the role of energy storage. The growing demand for storage solutions to support renewable energy and improve grid stability has led to an increased focus on optimal storage planning. In their work, Wogrin et al. [8] propose optimizing storage operations for medium- and long-term power system models, focusing on energy storage's potential to enhance grid reliability. Likewise, Akhavan and Mohsenian [11] present a chance-constrained optimization model for energy storage planning in active distribution grids, using non-parametric probability functions to account for uncertainties in energy supply and demand. These models assist in determining optimal locations and capacities for storage systems that support both grid stability and distributed energy sources. The role of electric vehicles in distribution system planning is another important consideration. The rise of electric vehicles (EVs) poses both challenges and opportunities for power distribution systems. The need to plan for EV charging stations (EVCS) is a significant aspect of expansion strategies, as they can place additional load on the grid and impact the distribution network's reliability. Liu et al. [13] discuss optimal planning for EVCS in distribution systems, focusing on the coordination of EV charging with DG to minimize impact on the existing network. A multi-objective planning approach that includes EV charging infrastructure and distributed generation is explored by Liu et al. [14], highlighting the need to balance these factors to achieve efficient network expansion. Moreover, studies have emphasized the integration of stochastic models to handle the uncertainties associated with EV charging and renewable energy. Weifeng et al. [16] propose a scenario-based comprehensive expansion planning approach that integrates EVs with distribution systems, considering the variability and uncertainty of EV charging patterns. Similarly, Zare et al. [17] develop a stochastic MILP model to address the expansion of multi-energy distribution networks with EV charging stations, showing how uncertainty can be incorporated into planning models to improve the robustness of the system. Incorporating energy storage and EV infrastructure into the distribution system also calls for attention to the reliability of the network. The planning models must address not only the capacity but also the resilience of the system under different operational scenarios. Sedghi et al. [9] focus on optimal storage planning in active distribution networks, considering the uncertainty of wind power distributed generation. Their work underscores the need to account for both generation and storage in planning to ensure system reliability under variable conditions. A holistic approach to expansion strategies involves considering the interplay between distributed generation, energy storage, and EV infrastructure, with a focus on achieving an optimal balance between these components. Yao et al. [15] discuss a multi-objective collaborative planning strategy for integrated power distribution and EV charging systems, highlighting the need for coordination to achieve optimal system performance. another crucial aspect of expansion planning is the role of demand-side management, which includes strategies such as demand response and energy efficiency programs. These programs play an essential role in optimizing the utilization of available resources and reducing the need for extensive infrastructure investments. Asensio et al. [7] present a stochastic programming model for joint distribution network and renewable energy expansion, incorporating demand response and energy storage. Their research emphasizes how demand-side management, when integrated with renewable energy and storage, can significantly enhance the flexibility and reliability of the distribution system. Moreover, the incorporation of electric vehicles (EVs) introduces a new layer of complexity in distribution system planning. As more EVs are integrated into the grid, there is a growing need to balance the increased demand for charging with the available capacity of the distribution network. Liu et al. [19] address this challenge by proposing a unified planning model that integrates distributed generation, EV charging stations, and the management of uncertainties such as battery degradation and fluctuating energy demands. This comprehensive approach aims to mitigate the impacts of EVs on the network while also ensuring that the system is adequately prepared for future demand. The expansion planning process is further complicated by the need to evaluate the hosting capacity of distribution networks, especially as new technologies like microgrids and EV charging stations become more prevalent. Da Silva et al. [23] explore the simultaneous assessment of distributed generation and electric vehicle hosting capacity in distribution systems. Their study provides insights into how to effectively evaluate and optimize the hosting capacity of these new technologies without compromising the reliability of the network.

The optimization of multi-energy systems is another emerging trend in the expansion of power distribution networks. Yuvaraj et al. [20] investigate the allocation of hydrogen-fuel-cell-based distributed generation in distribution systems to mitigate the impact of EV charging stations. They emphasize how multi-energy solutions can be used to enhance the reliability and sustainability of power distribution networks by diversifying energy sources and reducing dependence on conventional power generation. In line with these efforts, the integration of electric vehicles into the power distribution system also raises questions about the long-term sustainability of these technologies. Liu et al. [21] provide a comprehensive review and analysis of the allocation of electric vehicle charging stations in distribution networks, offering valuable insights into how these systems can be optimized to improve system performance while maintaining grid stability. Their work highlights the need for careful planning and coordination to ensure that the increase in EV charging infrastructure does not adversely impact the distribution network. Moreover, the incorporation of distributed energy resources (DERs) and electric vehicle charging stations calls for advanced planning models that consider multiple uncertainties, including weather patterns, electricity prices, and technological advancements. Akhavan and Mohsenian [11] discuss energy storage planning with non-parametric probability functions to optimize storage capacities while accounting for these uncertainties. The flexibility offered by such models allows for more robust and adaptive planning, which is crucial as the energy landscape continues to evolve. Additionally, the

optimization of storage systems, particularly in the context of active distribution grids, is gaining significant attention. Shen et al. [10] explore the role of centralized and distributed energy storage systems in the expansion planning of active distribution networks. Their work demonstrates how storage can be strategically integrated to enhance the stability and reliability of the grid, particularly during periods of high demand or low renewable generation. The use of both centralized and distributed storage systems offers a more flexible and resilient approach to power distribution system planning. Furthermore, optimizing the operations of battery energy storage systems and integrating them with renewable energy sources and EV charging stations can lead to substantial improvements in grid reliability. Li et al. [24] discuss the efficient operation of battery energy storage systems in conjunction with renewable energy sources and electric vehicle charging stations, demonstrating the potential for these systems to reduce operational costs while improving grid stability. Li et al. [25] proposed a mixed-integer linear programming (MILP) method for optimal planning of EVCS in urban power and transportation systems. Their approach focuses on optimizing the integration of EV charging infrastructure while considering both power system constraints and transportation network dynamics. Aljafari et al. [26] explore the optimization of radial distribution systems with the integration of distributed generation (DG) and EV charging stations. They employed a novel optimization technique called the Spotted Hyena Algorithm to tackle the complexities of balancing power supply and demand in the presence of DG and EV charging infrastructure. Yaghoubi-Nia et al. [27] focus on the optimized allocation of microgrids' distributed generation and EVCS, taking into account system uncertainties through clustering algorithms. Their work emphasizes the challenges of managing uncertainties in renewable generation and EV charging demand. By applying clustering techniques, they were able to group similar operational scenarios and optimize the allocation of DG and EVCS within the microgrid framework.

1.1. Contributions

- A unified multi-objective stochastic MILP model for the co-expansion of distribution networks, integrating DG units, ESS, and EVCS.
- A novel scenario generation and reduction framework that jointly models the uncertainties of renewable generation (wind/PV), conventional load, and EV charging demand based on travel patterns.
- A comprehensive analysis demonstrating that strategic DG investment can technically and economically defer traditional substation expansion.
- Validation on standard test networks showing the scalability of the proposed model and the impact of EV adoption on expansion plans.

2. Literature Review

In recent years, some models developed for unit commitment in power systems have been solved within a centralized framework. These models address optimal unit commitment scheduling. The expansion of distribution networks through reconfiguration and the addition of feeders strengthens existing grids and creates new networks [2]. In [3], a review of the current situation in the context of DSEP (Distribution System Expansion Planning) has been presented. The increasing penetration of DG (Distributed Generation), which is based on renewable energy sources, requires integration into distribution system planning models for decision-making regarding their location and timing [4]- [7]. Additionally, the uncertainty in the forecast of RES (Renewable Energy Sources) is usually considered unpredictable, and this uncertainty is addressed within the models. In [4], the uncertainty related to demand and DG is handled based on theoretical multi-scenario models executed using a genetic algorithm. In [5], the uncertainty associated with load and electricity prices is modeled via Monte Carlo simulation. In [6], a stochastic programming framework based on scenario analysis is used to minimize the present value of expected investment costs. Furthermore, the operational costs under uncertainty in DSEP are evaluated using dynamic programming in [7], where the response to demand and ESS (Energy Storage Systems) is also considered in the developed unit commitment planning model for distribution system planning and generation optimization. Other studies have explored the operational planning of ESS (Energy Storage Systems). In [8], the concept of a system, in contrast to load level, is expressed through time-series curves (as introduced in [6], [7]). This framework allows for the integration of better temporal information. In [9], optimal operational planning for batteries in distribution networks is implemented using heuristic methods, incorporating probability distributions to account for input variations. In [10], a multi-stage framework for unit commitment planning is proposed, where typical daily scenarios are used for hourly evaluations. The economic dispatch of ESS considers the impact of EVs (Electric Vehicles) in joint distribution, production, and planning of ESS expansion, excluding installation costs in EVCS (Electric Vehicle Charging Stations) [11]. A non-parametric, constrained optimization is employed for investment optimization in ESS units, considering the uncertainty in DG (Distributed Generation) and EV systems. In [12], a multi-objective optimization for battery storage and DG units in a distribution network is presented, where the power specifications of EVs are modeled using phase parameters for the design of the network system. Recently, there has been increasing attention given to the optimization of EVCS (Electric Vehicle Charging Stations) planning. In [13], the optimization of EVCS within distribution systems has been developed, with the goal of at least meeting the expansion needs. The costs involved are discussed in [14], where a mixed multi-objective model is proposed for planning, with an emphasis on new suggestions for replacing network assets, EVCS, and infrastructure. In [15], a multi-objective planning model for a distribution network, including DG (Distributed Generation) and EVCS, has been developed. An expansion scenario for distribution systems is proposed in [16], which takes into account the integration of EVs, with simultaneous charging and charging states. Table 1 compares recent studies and references over the past years [2]- [16], highlighting the present study.

Table 1. Dispersion of each dataset

Method	Network expansion	Expansion of renewable resources	Storage expansion	EV Charging station expansion
[2]	✓	-	-	-
[3-6]	✓	✓	-	-
[7]	✓	✓	✓	-
[8]	-	-	✓	-
[9]	✓	-	-	-
[10]	-	-	✓	-
[11]	-	✓	✓	-
[12]	-	-	-	✓
[13]	✓	-	-	✓
[14]	✓	✓	-	✓
[15]	✓	-	-	-
Proposed Study	✓	✓	✓	✓

3. Literature Review

In this section, the operation and limitations of the network expansion planning problem are discussed, considering the expansion of resources, substations, feeders, and key installations. For this purpose, all relevant computational models, including power flow calculations, reliability indices, and fuzzy numbers, should be provided before presenting the objective function and constraints. Additionally, since the problem under study involves a nonlinear and discrete mathematical model, as introduced in Section 1, the heuristic algorithm for optimization, such as the genetic algorithm, will be utilized to solve the problem

3.1. Distribution Flow Calculations in Distribution Networks

As is well known, in distribution networks, the ratio of R/X is much higher than that in transmission networks. This results in the non-convergence of methods used to calculate power flow in distribution networks, as opposed to transmission networks. Therefore, alternative methods have been proposed for these networks, with the most well-known and powerful being the backward and forward method, which can even be applied to networks with looped topologies. For this reason, this section introduces this method.

3.1.1 Backward and Forward Method

This method is based on two matrices that can be derived from the topology of the network. One matrix represents the branch flow in terms of path flow, and the other matrix represents the voltage drop across the path in terms of branch flow. The first matrix is referred to as matrix BIBC (Bus Injection to Branch Current), and the second matrix as matrix BCBV (Branch Current to Bus Voltage). The continuation of the process for constructing these two matrices is provided below.

1) Matrix of feeder current based on injection current at buses:

At each bus number i, the apparent power S_i given by the following equation (1):

$$S_i = (P_i + jQ_i).i = 1.2.\ldots.n \quad (1)$$

The number of buses: n

$$I_i^k = \left(\frac{P_i + jQ_i}{v_i^k}\right)^* .i = 1.2.\ldots.n \quad (2)$$

The voltage at bus I in the k-th iteration: v_i^k.

The current of the injection at bus i in the k-th iteration: I_i^k.

To construct this matrix (BIBC), a simple radial distribution system is presented as an example in Fig. 1. The injection current at the buses is calculated using the relationship in equation (2), and a system of current equations is written based on Kirchhoff's Current Law for the network. Therefore, the branch currents can be determined based on the injection current at the buses.

$$\begin{aligned} I_{S1} &= I_1 + I_2 + I_3 + I_4 \\ I_{S2} &= 2 \\ I_{S3} &= I_3 + I_4 \\ I_{s4} &= I_4 \end{aligned} \quad (3)$$

The current of the load at bus i: I_i.

The section current at bus i: I_{si}.

The system of equations (3) can be written in matrix form. This form is shown in relation (4).

$$\begin{bmatrix} I_{S1} \\ I_{S2} \\ I_{S3} \\ I_{S4} \end{bmatrix} = \begin{bmatrix} 1 & 1 & 1 & 1 \\ 0 & 1 & 0 & 0 \\ 0 & 0 & 1 & 1 \\ 0 & 0 & 0 & 1 \end{bmatrix} \begin{bmatrix} I_1 \\ I_2 \\ I_3 \\ I_4 \end{bmatrix} \quad (4)$$

Equation (4) can be written in the general form below:

$$[B] = [BIBC][I] \quad (5)$$

2) Voltage Matrix Based on Branch Current:

The relationship between branch currents and voltage across branches, for example, as shown in Fig. 1, is governed by Kirchhoff's voltage law in the form of the following equation:

$$\begin{aligned} V_1 &= V_0 - Z_1 I_{S1} \\ V_2 &= V_0 - Z_1 I_{S1} - Z_2 I_{S2} \\ V_3 &= V_0 - Z_1 I_{S1} - Z_3 I_{S3} \\ V_4 &= V_0 - Z_1 I_{S1} - Z_3 I_{S3} - Z_4 I_{S4} \end{aligned} \quad (6)$$

In this relation, V_0 represents the voltage at the branch terminal, which is a constant value. The equations (6) can be written in matrix form as:

Equation (7) can further be expressed in the general forms (8) or (9):

$$[V] = [V\_\cdot] = [BCBV][B] \quad (8)$$

$$[\Delta V] = [BIBV][B] \quad (9)$$

In this way, the voltage for each branch will be determined. What has been presented in equations (1) to (8) are the governing relations for the distribution network, which is based on radial flow. However, in order to perform the load flow calculations, as shown in equation (1), it is initially necessary to know the voltage at the buses, which is an unknown quantity. Therefore, the iterative method should be applied as follows:

Step 1: Initially, an assumed value for the voltage at all buses should be taken. For example, let Vi=1pu.

Step 2: Using equation (2), calculate the injection current for each bus.

Step 3: Using equation (4), calculate the branch currents.

Step 4: Using equation (8), calculate the voltage at each bus.

Step 5: If the calculated voltages show a significant difference from the previous voltage values, the algorithm should terminate. If not, proceed with the new voltages and return to Step 2.

This method typically converges to the solution after several iterations. By knowing the current in each branch, we will be able to calculate the losses.

3.1.2 Calculation of Losses

Although the total system losses are equal to the sum of the individual losses of the system components, which are calculated according to relation (10), instead of calculating the losses of each individual component, we can use the total active capacities at the load and power points. Active injection is applied to the system using the above distribution, which is calculated according to equation (11).

$$P_{loss} = real\left(\sum_{i=1}^{m} Z_i\, I_{si} I_{si}^*\right) \quad (10)$$

The number of branches: m

$$P_{loss} = real\left(S_{sunstation} - \sum_{i=1}^{m} S_i\right) \quad (11)$$

The number of buses: m

It should be noted that in the radial structure, in addition to the

above distribution path, there is a feeder for each path. Therefore, in the above relations, m=n. It is explained that equation (11) is computationally simpler than equation (10), but equation (10) is used to determine the percentage contribution of each branch in the overall system losses, which is useful for identifying weak branches for improvement or expansion.

3.2. Distribution Flow Calculations in Distribution Networks

In order to evaluate the reliability in distribution networks, which represents the level of reliability, indices are defined and calculated as alternative measures. The reliability indices in distribution networks are defined as:

1. SAIFI (System Average Interruption Frequency Index): The mean frequency of service interruptions for the system.
2. SAIDI (System Average Interruption Duration Index): The mean duration of service interruptions for the system.
3. CAIFI (Customer Average Interruption Frequency Index): The mean frequency of service interruptions for each customer.
4. CAIDI (Customer Average Interruption Duration Index): The mean duration of service interruptions for each customer.
5. ENS (Energy Not supplied): The energy not supplied.

Depending on the type of study, one or more of these indices may be used. Although calculating other indices, such as SAIFI, is easier in most studies, the goal is usually to improve both losses and reliability. Therefore, reliability indices are used to assess performance, which can be summed with weightage. In other words, the associated indices should include energy considerations. The necessary equations for calculating these indices include two main stages. In the first stage, the basic indices for each branch point are determined:

$$\lambda_s = \sum_{i=1}^{m} \lambda_i \qquad (\frac{f}{yr}) \tag{12}$$

$$U_s = \sum_{i=1}^{n} \lambda_i \, r_i \qquad (\frac{h}{yr}) \tag{13}$$

$$r_s = \frac{U_s}{\lambda_s} \qquad (\frac{h}{f}) \tag{14}$$

In this context, it is noted that since the distribution system is radial, similar to a series system, the failure rate for each load point is the sum of the failure rates of all devices located before that load point. The second stage involves calculating each of the reliability indices. Since this paper only uses the energy loss index, the calculation method for the ENS index is as follows:

$$ENS = \sum_{j=1}^{n} \sum_{i=1}^{m} \lambda_i \, r_{ij} P_j \tag{15}$$

Number of consumption buses: n;

Number of sections: m

Other indices are calculated in the following order:

$$\text{SAIFI} = \frac{Total\ number\ of\ subscriber\ disconnections}{Total\ number\ of\ subscribers} \tag{16}$$

$$SAIDI = \frac{Total\ times\ of\ subscriber\ disconnections}{Total\ number\ of\ subscribers} \tag{17}$$

$$CAIFI = \frac{Total\ times\ of\ subscriber\ disconnections}{Total\ number\ of\ affecte\ subscribers} \tag{18}$$

$$SCAIDI = \frac{Total\ times\ of\ subscriber\ disconnections}{Total\ number\ of\ subscriber\ disconnections} \tag{19}$$

If we want to consider each of the above indices along with the damages in the objective function, we must either assign appropriate weights to the damages in the objective function to ensure the associated index is computable or use risk management methods to extract and manage risk. The details of these methods are discussed in Section 5.

3.3 Modeling Uncertainty in Renewable Sources

The scenario-based method is one of the common techniques used for modeling uncertainty. Then, using the probability distribution function, the likelihood of assigning an undefined parameter to each section of the divided curve is calculated. Each section of the curve corresponds to a scenario. For example, the curve is divided into k sections (scenarios), with the probability of each section denoted by Pk. Therefore, the expected value of the undefined parameter is represented as:

$$y = \sum_{i=1}^{K} P_i \; X_i \tag{20}$$

It should be noted that an increased number of scenarios improves the accuracy of the solution method, but it also increases the computational burden.

3.3.1 Relationship Between Uncertainty and Fluctuations in the Generation of Renewable Sources

To demonstrate the uncertainty in this section, the standard deviation (σ) and the predicted value of renewable energy generation, which includes generation fluctuations (μ), have been used. The relationship between these two parameters, based on measurement values and tests (as shown in Fig. 3), is described by the equation (21). The tests were conducted such that the predicted average wind speed for a given year, over several hours, resulted in scenarios that deviated significantly from the predicted average. In cases with lower average wind speed, the actual wind speed was very close to the predicted average, and after increasing the number of tests for each predicted wind speed, the standard deviation was calculated.

$$\sigma = 0.231 + 0.197\ \mu \tag{21}$$

As observed from the relationship, for wind sources, the level of uncertainty is higher, and there is a strong correlation with the predicted average wind speed. This means that at higher wind speeds, the level of uncertainty increases by a factor of 0.197, while for solar energy sources, the uncertainty is lower than the predicted value.

3.3.2 Generation of Scenarios for Modeling Uncertainty

To model the uncertainty in renewable energy sources for evaluating the reliability of power systems, the first step involves generating a multi-state model for these sources across different hours for short-term studies or across different seasons for long-term studies. This modeling approach can be executed using a new scenario generation method, referred to as LHS (Latin Hypercube Sampling).

3.3.2.1 Probabilistic Wind Turbine Model

Since wind turbine units are renewable, they provide rotational energy. Previous research has shown that wind speed characteristics in a particular location have the highest correlation with a Weibull distribution. Therefore, in this study, we assume that the wind speed follows a Weibull distribution with the mean wind speed as the reference. The probabilistic description of wind speed using a Weibull distribution is provided as follows:

$$f(v) = \left(\frac{k}{c}\right)\left(\frac{v}{c}\right)^{(k-1)} \; e^{-(\frac{v}{c})^k} \quad 0 < v < \infty \tag{22}$$

In this, *v*, *k*, and *c* represent the wind speed (in m/s or miles/h), the shape factor (dimensionless), and the scale factor (fraction of the reference wind speed), respectively.

For simplicity, the wind speed distribution is normalized by the mean wind speed $vmean$using a Weibull distribution. Probable values from v_{mean} are considered for a fixed increase until the majority of the distribution is encompassed.

3.3.2.2 Probabilistic Photovoltaic Model

The photovoltaic (PV) output primarily depends on solar irradiation. Since irradiation levels vary throughout the day, PV systems, like wind turbines, are classified as renewable energy sources. The hourly distribution of solar irradiation at a specific location typically follows a bimodal distribution, which can be represented as a linear combination of two uni-modal distributions. Uni-modal distribution functions can be modeled using Beta, Weibull, and log-normal distributions. In this study, a bimodal distribution is used based on Equation (2):

$$f(g) = \omega\left(\frac{k_1}{c_1}\right)\left(\frac{g}{c_1}\right)^{(k_1-1)} e^{-\left(\frac{g}{c_1}\right)^{k_1}} + (1-\omega)\left(\frac{k_2}{c_2}\right)\left(\frac{g}{c_2}\right)^{(k_2-1)} e^{-\left(\frac{g}{c_2}\right)^{k_2}} \quad (23)$$
$$. 0 < g < \infty$$

where g represents solar irradiation (in kW/m²), ω denotes the weighting factor, k_1 and k_2 are the shape factors, and c_1 and c_2 are the scale factors.

3.4 Probabilistic Photovoltaic Model

The objective function of this problem is presented by equation (24-3), where the current value of the total network cost is minimized.

$$min = \left\{\sum_t \frac{(1+I)^{-t}}{I} c_t^I + \left[\sum_t (1+I)^{-t}(c_t^M + c_t^E + c_t^R + c_t^U) + \frac{(1+I)^{-n_T}}{I}\left(c_{n_T}^M + c_{n_T}^E + c_{n_T}^R + c_{n_T}^U\right)\right]\right\} \quad (24)$$

which is given by:

$$c_t^I = \sum_{l\in\{NRF.NAF\}} RR^l \sum_{k\in K^l}\sum_{(i.j)\in\gamma^l} C_k^{I.l}\ell_{ij}x_{ijkt}^l + RR^{SS}\sum_{i\in\Omega^{SS}} C_i^{I.SS}x_{it}^{SS} + RR^{NT}\sum_{k\in K^{NT}}\sum_{i\in\Omega^{SS}} C_k^{I.NT}x_{ikt}^{NT} + \sum_{p\in P} RR^p \sum_{k\in K^p}\sum_{i\in\Omega^p} C_k^{I.p}pf\bar{G}_k^p x_{ikt}^p + RR^{ST}\sum_{k\in K^{ST}}\sum_{i\in\Omega^{ST}} C_k^{I.ST}pf\bar{G}_k^{ST}x_{ikt}^{ST} + \sum_{ch\in CH} RR^{ch}\sum_{k\in K^{ch}}\sum_{i\in\Omega^{ST}} C_k^{I,ch}pf\bar{G}_k^{ch}x_{ikt}^{ch};\ \forall t\in T \quad (25)$$

$$c_t^M = \sum_{l\in L}\sum_{k\in K^l}\sum_{(i,j)\in Y^l} C_k^{M,l}\left(y_{ijkt}^l + y_{jikt}^l\right) + \sum_{tr\in TR}\sum_{k\in K^{tr}}\sum_{i\in\Omega^{ss}} C_k^{M,tr}y_{ikt}^{tr} + \sum_{p\in P}\sum_{k\in K^p}\sum_{i\in\Omega^p} C_k^{M,p}y_{ikt}^p + \sum_{k\in K^{ST}}\sum_{i\in\Omega^{ST}} C_k^{M,ST}y_{ikt}^{ST} + \sum_{ch\in CH}\sum_{k\in K^{ch}}\sum_{i\in\Omega^{ch}} C_k^{M,ch}y_{ikt}^{ch};\ \forall t\in \mathrm{T} \quad (26)$$

$$c_t^E = \sum_{q\in Q}\sum_{b\in B}\sum_{\omega\in\Pi}\pi_{qb\omega}\Delta_{qb}pf \left(\sum_{tr\in TR}\sum_{k\in K^{tr}}\sum_{i\in\Omega^{SS}} C_{tqb\omega}^{SS}g_{iktqb\omega}^{tr} + \sum_{p\in P}\sum_{k\in K^p}\sum_{i\in\Omega^p} C_k^{E.p}g_{iktqb\omega}^p + \sum_{k\in K^{ST}}\sum_{i\in\Omega^{ST}} C_k^{ST.prod}g_{iktqb\omega}^{ST.prod} + \sum_{k\in K^{ST}}\sum_{i\in\Omega^{ST}} C_k^{ST.\,\mathrm{store}}g_{iktqb\omega}^{ST.\,\mathrm{store}}\right);\forall t\in T \quad (27)$$

$$c_t^R = \sum_{q\in Q}\sum_{b\in B}\sum_{\omega\in\Pi}\pi_{qb\omega}\Delta_{qb}C_{tqb\omega}^{SS}pf \left(\sum_{tr\in TR}\sum_{k\in K^{tr}}\sum_{i\in\Omega^{SS}} Z_k^{tr}\left(g_{iktqb\omega}^{tr}\right)^2 + \sum_{l\in L}\sum_{k\in K^l}\sum_{(i.j)\in\Upsilon^l} Z_k^l\ell_{ij}\left(f_{ijktqb\omega}^l + f_{jiktqb\omega}^l\right)^2\right); \forall t\in T \quad (28)$$

$$c_t^U = \sum_{q\in Q}\sum_{b\in B}\sum_{\omega\in\Pi}\pi_{qb\omega}\Delta_{qb}C^U pf\sum_{i\in\Omega_t^{LN}} d_{itqb\omega}^U;\forall t\in T \quad (29)$$

The objective function consists of three parts. The first part represents the current value of the investment cost. This cost is incurred over the lifetime of each device, which has been replaced. It is assumed that after the end of each device's lifetime in the planning horizon, a replacement device will be installed. The second component represents the current value of the operating cost, and finally, the third component of the objective function (24) represents the operating cost after the final stage of the planning horizon, assuming that these devices must continue to operate until the end of their lifetime. The investment cost is described by equation (25), the maintenance cost by equation (26), the production cost by equation (27), the energy loss cost by equation (28), and the energy supply cost by equation (29). The rate of return on investment is calculated using equation (30), which depends on the lifetime of each device.

$$RR^a = \frac{I(1+I)^{v^a}}{((1+I)^{v^a-1})} \quad (30)$$

3.4.2 Constraints

Initially, the technical constraints of the network, such as the operating laws and the limitations on the utilization of devices, are presented. Equation (31) represents the power or current balance in each branch. The Kirchhoff voltage law is also expressed by equation (32). Equation (33) presents the voltage constraint for each branch. Equations (34) to (37) describe the current limits for the feeders and the production capacity constraints for the power generation units. Equation (38) presents the limitation on the penetration of renewable energy sources, expressed as a percentage of the total network load.

$$\sum_{l\in L}\sum_{k\in K^l}\sum_{j\in\Omega_i^l}\left(f_{ijktqb\omega}^l - f_{jiktqb\omega}^l\right) = \sum_{tr\in TR}\sum_{k\in K^{tr}} g_{iktqb\omega}^{tr} + \sum_{p\in P}\sum_{k\in K^p} g_{iktqb\omega}^p + \sum_{k\in K^{st}} g_{iktqb\omega}^{ST.prod} - \sum_{k\in K^{st}} g_{iktqb\omega}^{ST.store} - D_{iktqb\omega} - d_{itqb\omega}^U - d_{itqb\omega}^{CH}: \forall i\in\Omega^N.\forall t\in T.\forall q\in Q.\forall b\in B.\forall\omega\in\Pi \quad (31)$$

$$y_{ijkt}^l\left[Z_{ijk}^l \ell_{ij} f_{ijktqb\omega}^l - \left(v_{itqb\omega} - v_{jtqb\omega}\right)\right] = 0; \forall l\in L.\ \forall i\in\Omega_j^l.\forall j\in\Omega^N.\forall k\in K^l \forall t\in T.\forall q\in Q.\forall b\in B.\forall\omega\in\Pi \quad (32)$$

$$\underline{V} \le v_{itqb\omega} \le \bar{V}; \forall i\in\Omega^N.\forall t\in T.\forall q\in Q.\forall b\in B.\forall\omega\in\Pi \quad (33)$$

$$0 \le f_{ijktqb\omega}^l \le y_{ijkt}^l \bar{F}_{ijk}^l; \forall l\in L.\forall i\in\Omega_j^l.\forall j\in\Omega^N.\forall k\in K^l. \forall t\in T.\forall q\in Q.\forall b\in B.\forall\omega\in\Pi \quad (34)$$

$$0 \le g_{iktqb\omega}^{tr} \le y_{ikt}^{tr}\bar{G}_k^{tr}; \forall tr\in TR.\forall i\in\Omega^{SS}.\forall j\in\Omega^N.\forall k\in K^{NT}. \quad (35)$$

$$\forall t\in T.\forall q\in Q.\forall b\in B.\forall\omega\in\Pi \quad 0 \le g_{iktqb\omega}^p \le y_{ikt}^p \hat{G}_{iktqb\omega}^p; \forall p\in P.\forall i\in\Omega^p.\forall k\in K^p. \forall t\in T.\forall q\in Q.\forall b\in B.\forall\omega\in\Pi \quad (36)$$

$$0 \le d_{itqb\omega}^U \le d_{itqb\omega} + d_{itqb\omega}^{CH}; \forall i\in\Omega^N.\forall t\in T.\forall q\in Q.\forall b\in B.\forall\omega\in\Pi \quad (37)$$

$$\sum_{p\in P}\sum_{k\in K^p}\sum_{i\in\Omega^p} g_{iktqb\omega}^p + \sum_{k\in K^{ST}}\sum_{i\in\Omega^{ST}}\left(g_{iktqb\omega}^{ST.prod} - g_{iktqb\omega}^{ST.store}\right) \le \varepsilon\left(\sum_{i\in\omega_t^{L_N}} D_{itqb\omega} + d_{itqb\omega}^{cH}\right); \forall t\in T.\forall q\in Q.\forall b\in B.\forall\omega\in\Pi \quad (38)$$

The amount of charging or discharging power of the energy storage system is limited by its capacity, as modeled in equations (39) to (40). Additionally, at any given moment, the energy storage system can only be in one of two states: charging or discharging, which is described in equation (41).

$$\underline{G}_k^{ST} u_{iktqb\omega}^{ST.prod} \le g_{iktqb\omega}^{ST.prod} \le \bar{G}_k^{ST.prod} u_{iktqb\omega}^{ST.prod}; \forall i\in\Omega^{ST}.\forall k\in K^{ST}.\forall t\in T.\forall q\in Q.\forall b\in B.\forall\omega\in\Pi \quad (39)$$

$$G_k^{ST} u_{iktqb\omega}^{ST.\,\text{store}} \le g_{iktqb\omega}^{ST.\,\text{store}} \le \bar{G}_k^{\text{ST,prod}} u_{iktqb\omega}^{ST.\,\text{store}}; \forall i\in\Omega^{ST}.\forall k\in K^{ST}.\forall t\in T.\forall q\in Q.\forall b\in B.\forall\omega\in\Pi \quad (40)$$

$$u_{iktqb\omega}^{ST,prod} + u_{iktqb\omega}^{ST,\,\text{store}} \le y_{ikt}^{ST}; \forall i\in\Omega^{ST}.\forall k\in K^{ST}.\forall t\in T.\forall q\in Q.\forall b\in B.\forall\omega\in\Pi \quad (41)$$

The constraint on investment and the use of each device is described in equations (42) to (47). In equations (48) and (49), the new transformers, in the case of the expansion of the charging station in the previous phase, will be added to the system.

$$\sum_{t\in T}\sum_{k\in K^l} x_{ijkt}^l \le 1; \forall l\in\{NRF.NAF\}.\forall(i.j)\in\Upsilon^l \quad (42)$$

$$\sum_{t\in T} x_{it}^{SS} \le 1; \forall i\in\Omega^{SS} \quad (43)$$

$$\sum_{t\in T}\sum_{k\in K^{NT}} x_{ikt}^{NT} \le 1; \forall i\in\Omega^{SS} \quad (44)$$

$$\sum_{t\in T}\sum_{k\in K^p} x_{ikt}^p \le 1; \forall p\in P.\forall i\in\Omega^p \quad (45)$$

$$\sum_{t\in T}\sum_{k\in K^{ST}} x_{ikt}^{ST} \le 1; \forall i\in\Omega^{ST} \quad (46)$$

$$\sum_{t\in T}\sum_{k\in K^{ch}} x_{ikt}^{ch} \le 1; \forall ch\in CH.\forall i\in\Omega^{ch} \quad (47)$$

$$x_{ikt}^{NT} \le \sum_{\tau=1}^{t} x_{i\tau}^{SS}; \forall i\in\Omega^{SS}.\forall k\in K^{NT}; \forall t\in T \quad (48)$$

$$x_{ikt}^{ACH} \le \sum_{\tau=1}^{t} x_{ik\tau}^{NCH}; \forall i\in\Omega^{ACH}.\forall k\in K^{ACH}; \forall t\in T \quad (49)$$

Equations (50) to (52) model the operation of utilizing new feeders and existing feeders by specifying the direction of flow in each feeder. In fact, equation (52) makes the use of an existing feeder impossible in the case of replacing a feeder. Additionally, the possibility of utilizing new transformers, new generators, batteries, electric vehicles, and charging stations is modeled in equations (53) to (56).

$$y_{ijkt}^{EFF} + y_{jikt}^{EFF} \le 1; \forall(i.j)\in\Upsilon^{EFF}.\forall k\in K^{EFF}.\forall t\in T \quad (50)$$

$$y_{ijkt}^l + y_{jikt}^l \le \sum_{\tau=1}^{t} x_{ijk\tau}^l; \forall l\in\{NRF.NAF\}.\forall(i.j)\in\Upsilon^l.\forall k\in K^l.\forall t\in T \quad (51)$$

$$y_{ijkt}^{ERF} + y_{jikt}^{ERF} \le 1 - \sum_{\tau=1}^{t}\sum_{\kappa\in K^{NRF}} x_{ijk\tau}^{NRF}; \forall(i.j)\in\Upsilon^{ERF}.\forall k\in K^{ERF}.\forall t\in T \quad (52)$$

$$y_{ikt}^{NT} \le \sum_{\tau=1}^{t} x_{ik\tau}^{NT}; \forall i\in\Omega^{\text{SS}}.\forall k\in K^{NT}.\forall t\in T \quad (53)$$

$$y_{ikt}^{ST} \le \sum_{\tau=1}^{t} x_{ik\tau}^{ST}; \forall i\in\Omega^{\text{ST}}.\forall k\in K^{ST}.\forall t\in T \quad (54)$$

$$y_{ikt}^{ST} \le \sum_{\tau=1}^{t} x_{ik\tau}^{ST}; \forall i\in\Omega^{\text{ST}}.\forall k\in K^{ST}.\forall t\in T \quad (55)$$

$$y_{ikt}^{ch} \le \sum_{\tau=1}^{t} x_{ikt}^{ch}; \forall ch\in CH.\forall i\in\Omega^{ch}.\forall k\in K^{ch}.\forall t\in T \quad (56)$$

In equation (56), the total investment amount at each stage is

limited to the budget of each stage.

$$\sum_{l\in\{NRF,NAF\}}\sum_{k\in K^l}\sum_{(ij)\in Y^{\wedge}l} C_k^{I.}\ell_{ij}x_{ijkt}^{l} + \sum_{i\in\Omega^{SS}} C_i^{I.SS}x_{it}^{SS} + \sum_{k\in K^{NT}}\sum_{i\in\Omega^{SS}} C_k^{I.NT}x_{ikt}^{NT} + \sum_{p\in P}\sum_{i\in\Omega^{p}} C_k^{I.p}pf\bar{G}_k^{p}x_{ikt}^{p} + \sum_{p\in P}\sum_{i\in\Omega^{ST}} C_k^{I.ST}pf\bar{G}_k^{ST}x_{ikt}^{ST} + \sum_{ch\in CH}\sum_{i\in\Omega^{ch}} C_k^{I.ch}pf\bar{G}_k^{ch}x_{ikt}^{ch} \le IB_t;\forall t\in T \quad (57)$$

In order to achieve a distributed configuration, equation (57) allows only one flow entry path per load group. In equation (58), other groups are also restricted to a flow entry from only one branch. Constraints (59) to (67) prevent the disconnection of generators, which must be implemented through the load and network in case of necessity.

$$\sum_{l\in L}\sum_{i\in\Omega_j^{l}}\sum_{k\in K^l} y_{ijkt}^{l} = 1;\forall j\in\Omega_t^{LN}.\forall t\in T \quad (58)$$

$$\sum_{l\in L}\sum_{i\in\Omega_j^{l}}\sum_{k\in K^l} y_{ijkt}^{l} \le 1;\forall j\notin\Omega_t^{LN}.\forall t\in T \quad (59)$$

$$\sum_{l\in L}\sum_{k\in K^l}\sum_{j\in\Omega_i^{l}}\left(\tilde{f}_{ijkt}^{l}-\tilde{f}_{jikt}^{l}\right) = \tilde{g}_{it}^{SS}-\widetilde{D}_{it};\forall i\in\Omega^{N}.\forall t\in T \quad (60)$$

$$0\le\tilde{f}_{ijkt}^{EFF}\le n_{DG};\forall i\in\Omega_j^{EFF}.\ \forall j\in\Omega^{N}.\forall k\in K^{EFF}.\forall t\in T \quad (61)$$

$$0\le\tilde{f}_{ijkt}^{ERF}\le\left(1-\sum_{\tau=1}^{t}\sum_{\kappa\in K^{NRF}} x_{ijk\tau}^{NRF}\right)n_{DG};\ \forall(i.j)\in\Upsilon^{EFF}.\forall k\in K^{ERF}.\forall t\in T \quad (62)$$

$$0\le\tilde{f}_{jikt}^{ERF}\le\left(1-\sum_{\tau=1}^{t}\sum_{\kappa\in K^{NRF}} x_{ijk\tau}^{NRF}\right)n_{DG};\ \forall(i.j)\in\Upsilon^{EFF}.\forall k\in K^{ERF}.\forall t\in T \quad (63)$$

$$0\le\tilde{f}_{ijkt}^{l}\le\left(\sum_{\tau=1}^{t} x_{ijk\tau}^{l}\right)n_{DG};; \quad \forall l\in\{NRF.NAF\}.\forall(i.j)\in\Upsilon^{l}.\forall k\in K^{l}.\forall t\in T \quad (64)$$

$$0\le\tilde{f}_{jikt}^{l}\le\left(\sum_{\tau=1}^{t} x_{ijk\tau}^{l}\right)n_{DG};\ \forall l\in\{NRF.NAF\}.\forall(i.j)\in\Upsilon^{l}.\forall k\in K^{l}.\forall t\in T \quad (65)$$

$$0\le\tilde{f}_{ijkt}^{ERF}\le\left(1-\sum_{\tau=1}^{t}\sum_{\kappa\in K^{NRF}} x_{ijk\tau}^{NRF}\right)n_{DG};\ \forall(i.j)\in\Upsilon^{EFF}.\forall k\in K^{ERF}.\forall t\in T \quad (66)$$

$$0\le\tilde{g}_{it}^{SS}\le n_{DG};\forall i\in\Omega^{SS}.\forall t\in T \quad (67)$$

$$\widetilde{D}_{it}=\begin{cases}1;\forall i\in\Omega_t^{LN}.\forall t\in T\\ 0;\forall i\notin\Omega_t^{LN}.\forall t\in T\end{cases} \quad (68)$$

transfer limitation in 15-minute intervals is modeled in equation (68).

$$\sum_{b}\left[\Delta_{qb}\left(\eta_i^{ST.\,\text{store}}\,g_{\text{iktqb}\,\omega}^{ST.\,\text{store}}-\left(\frac{1}{\eta_i^{ST.prod}}\right)g_{\text{iktqb}\,\omega}^{ST.prod}\right)\right] = 0;\forall i\in\Omega^{ST}.\forall k\in K^{ST}.\ \forall t\in T.\forall q\in Q.\forall\omega\in\Pi \quad (69)$$

Finally, equations (69) and (70) define the power capacity constraints for the electric vehicles in each group and across the entire network, respectively.

$$0\le d_{itqb\omega}^{ch}\le\bar{G}_k^{ch}y_{ikt}^{ch}; \quad (69)$$

$$\sum_{ch\in CH}\sum_{i\in\Omega^{cH}} d_{itqb\omega}^{ch} = \text{dem}_{tqb\omega}^{EV};\forall t\in T.\forall b\in B.\forall q\in Q.\forall\omega\in\Pi \quad (70)$$

3.5 Equipment Model

In the previous section, the performance and limitations of the network expansion problem were studied. In the objective functions and constraints of the problem, governing equations for production, load balance, and other components for generation sources and storage systems were provided. In this section, a detailed model for the production of wind, solar, and electric vehicles is presented. It should be noted that the governing equations for storage devices are equations (10) and (11). It is important to know the amount of hydrogen at each pressure that is converted into a specific amount of electrical energy.

3.5.1 Wind Source

Considering the wind speed distribution and the relation between wind speed and power, the power distribution of the wind turbine can be determined.

In the conclusion of this paper, the power conversion relationship is described as follows:

$$\omega=\begin{cases}0. & \text{for } v<v_i \text{ and } v>v_o\\ \dfrac{\omega_r(v-v_i)}{(v_r-v_i)}. & \text{for } v_i\le v\le v_r\\ \omega_r. & \text{for } v_r\le v\le v_o\end{cases} \quad (71)$$

In which ω, ω_r, v_i, v_r, and $v_o$represent the output power of the wind turbine (kW), rated power, minimum wind speed, rated wind speed, and maximum wind speed, respectively.

3.5.2 Thermal Power Source

Considering the distribution of radiation and the conversion of radiation to power, the distribution of PV power can be obtained. The conversion of radiation to power used in this paper is expressed as:

$$p=\eta^{PV}S^{PV}g \quad (72)$$

Where p represents the output power of the PV system (kW), η^{PV} denotes the efficiency (%), and S^{PV} refers to the total area of the PV system (m²).

3.5.3 Electric Vehicles

Here, the objective functions defined in the previous section remain unchanged, while only the constraints related to line current limits and bus voltage levels are added to the network from this section. The subsequent sections will present the exact mathematical model for these loads.

The objective of this study is to determine the charging and discharging rates of electric vehicles (EVs) in a radial distribution network. It is assumed that the charging and discharging rates of EVs are centrally controlled and can be adjusted to any possible value within a given continuous range. The energy stored in the vehicle battery, measured in kilowatt-hours (kWh), is used as an indicator of

the battery's state of charge. The stored energy in the battery of vehicle k-th at time t must satisfy condition (73).

Additionally, the stored energy in a battery at each hour is calculated using equation (74).

$$0 \le s_k(t) \le s^{\max} \tag{73}$$

$$s_k(t) = s_k(t-1) + \tau V_{\text{nom}} x_{k.t} \Delta t. k \in \mathcal{K}. t \in \mathcal{T} \tag{74}$$

The voltage V_{nom} is the nominal voltage of the network, and $x_{k.t}$, is the current supplied to the vehicle. Δt is the time step of the discrete time intervals, and τ is the efficiency factor (we use 0.9 as a typical value) which accounts for the AC/DC current conversion and losses in the battery charging process. The voltage at the connection point is typically not more than 5% different from the nominal voltage.

A. Nominal Capacity of Transformers

Transformers have a nominal capacity of power, $P_{Tx}^{\max}$, which must be maintained within reasonable limits. Exceeding this capacity may cause a reduction in the transformer's lifespan. However, most transformers are designed to tolerate up to 130% of their nominal capacity $P_{Tx}^{\max}$, for a limited period before the cooling system stabilizes. This limit is defined based on a step-by-step analysis and can be expressed as:

$$V_{T.x} x_{\phi.t} \le \frac{1}{3} P_{Tx}^{\max} \times 130\%. \quad \phi \in \{A.B.C\} \tag{75}$$

B. Nominal Current Capacity of Lines

Electric lines have various limitations, the most important of which is the current capacity. If this capacity is exceeded, the cable may be damaged. Let us assume that cable i has a maximum capacity of $P_i^{\max}$. In the network under study, both the main lines and service lines typically have different technical specifications. Therefore, separate limitations are applied to each section of the main lines, and finally, individual limitations are applied to each service line in the network:

$$\begin{gathered} \text{Backbone: } x_{\phi.t} \le x_{\phi}^{\max}. \phi \in \{A.B.C\} \\ \text{Service Lines: } x_{k.t}^{\text{tot}} \le x_k^{\max}. \forall k \in \mathcal{K} \end{gathered} \tag{76}$$

C. Voltage Drop

The voltage must be maintained within upper and lower limits at every connection point. If these limits are not respected, the household loads may experience adverse effects.

Consider the simplified electrical network, where each load Si consists of a combination of household and electric vehicle loads, all of which are connected to a single phase. The total voltage drops, Vdrop, of the transformer at a household can be estimated by considering the equivalent circuit:

$$V_4^{\text{drop}} = (I_2 + I_3 + I_4) z_{12} + (I_3 + I_4) z_{23} + I_4 z_{34} \tag{77}$$

And typically, in house h

$$V_h^{\text{drop}} = \sum_{j=1}^{h} \left(I_j \sum_{k=1}^{j} z_{k-1.k} \right) \tag{78}$$

since I_j is a combination of the existing households and the electric vehicle load, and since we are modeling a network that primarily exhibits resistance, a linear expression will be obtained. The voltage limit in each house h and at each future time interval will be as follows:

$$0 \le s_k(t) \le s^{\max} \tag{79}$$

D. Battery

It is important to avoid exceeding the maximum battery capacity. This is expressed under the following condition:

In addition, these batteries have both a minimum and maximum charging current limit, which must be adhered to in order to protect the battery and ensure appropriate charging efficiency.

$$x^{\min} < x_{k.t} < x^{\max} \tag{80}$$

E. Charging Algorithms

Each vehicle has an algorithm to reach up to 95% of its maximum energy storage capacity within a limited time, denoted as Tk, starting from the moment charging begins:

$$S_{\text{k}}(0) + \sum_{t=0}^{T_k} \tau x_{k.t} V_{\text{nom}} \Delta t > 0.95 \times S^{\max} \tag{81}$$

3.6 Solution Method

As we know, optimization problems encompass a wide range of engineering challenges in power systems, especially in scheduling and operational studies. Therefore, the optimization of solution methods is one of the main challenges in power system engineering, depending on the type of problem (linear, nonlinear, continuous, discrete, etc.) and the required solution time (online or offline). Various methods have been proposed to address these issues. Considering the nature of multi-objective problems, optimization methods for multi-objective problems and the approach to selecting the optimal final solution are provided in the feasible solution space.

3.6.1 Multi-Objective Optimization

In general, optimization involves finding the best solution from a set of available options (considering the constraints of the problem), with the goal of optimizing a single or multiple objective. Multi-objective optimization problems are a Multi Criteria Decision Making (MCDM), where an optimal solution is obtained from a set of possible solutions. In these types of problems, unlike single-objective problems, due to the existence of multiple objectives, a set of possible solutions is obtained:

$$\min f(x) = \{f_1(x). \ldots . f_n(x)\} \tag{82}$$

$$\begin{gathered} g(x) \le 0 \\ h(x) = 0 \end{gathered} \tag{83}$$

When calculating each new response, it is necessary to assess whether it is better or worse compared to the existing responses. The concept of dominance is defined such that response A dominates response B if there is no response worse than A and at least one objective function is better for response A than for response B. If such a condition is met for a new response B, it is removed from the set of responses, otherwise, it is added to the set of existing responses.

The selection method follows the max-min rule as described in equation (84). In this method, the minimum objective function value is applied to each of the non-dominated responses to obtain the smallest possible objective value for each response. Hence, for each response, an objective function is chosen, and from these values, the maximum possible value is selected. This maximum value corresponds to each response from the set of non-dominated solutions. The chosen value is as follows:

$$\max \left(\min_k \{ f_{1.k}. f_{2.k}. \ldots . f_{np.k} \} \right. \tag{84}$$

In this relationship, k refers to the number of objectives and np refers to the number of responses in the Pareto front. The selection method with the ranking method is based on the objective functions according to equations (85) to (87). If the goal is to maximize the objective, equation (85) is used for normalization, and if the goal should be minimized, equation (86) is applied. After normalizing each objective for every response, a final membership function for each objective is obtained according to equation (87), which is used to determine the best possible response until an optimal solution is found.

$$\mu_i^k = \frac{f_i^{\max} - f_i^k}{f_i^{\max} - f_i^{\min}} \quad (85)$$

$$\mu_i^k = \frac{f_i^k - f_i^{\min}}{f_i^{\max} - f_i^{\min}} \quad (86)$$

$$\mu^k = \frac{\sum_{i=0}^{np} \mu_i^k}{\sum_{k=0}^{nk} \sum_{i=0}^{np} \mu_i^k} \quad (87)$$

In this paper, the max-min method will be used to select the final response. The overall flowchart of the proposed method is given in Fig. 1.

4. Results and Analysis

In order to assess the performance of the proposed algorithm, the model must be applied to a real system. In this section, the proposed model is applied to a system with a primary feeder, and the actions taken and the results of the study are presented. The stages of the study follow the steps of the proposed algorithm in a sequential manner. The results from each stage are provided and analyzed. Finally, considering that the present paper problem is a multi-objective problem, a Pareto space has been derived for different objectives that have been analyzed, and the optimal selection for the network is based on the technical and budgetary constraints and user preferences. The simulations are performed on a hardware with the following features: (PC with Intel i7 CPU, 16GB RAM).

4.1 Results and Analysis

As mentioned, the numerical studies in this paper have been conducted on two standardized radial distribution systems. Initially, the study was performed on a small and simple network, and then the proposed model was applied to a larger network. In order to demonstrate the impact of distributed generation sources and electric vehicles on the system expansion, the study was conducted on two systems in three scenarios, which include the following:

- First Scenario: Without considering the electric vehicles, solving the problem as a single-objective optimization.
- Second Scenario: Without considering the electric vehicles, solving the problem as a multi-objective optimization.
- Third Scenario: Considering the electric vehicles, solving the problem as a single-objective optimization.

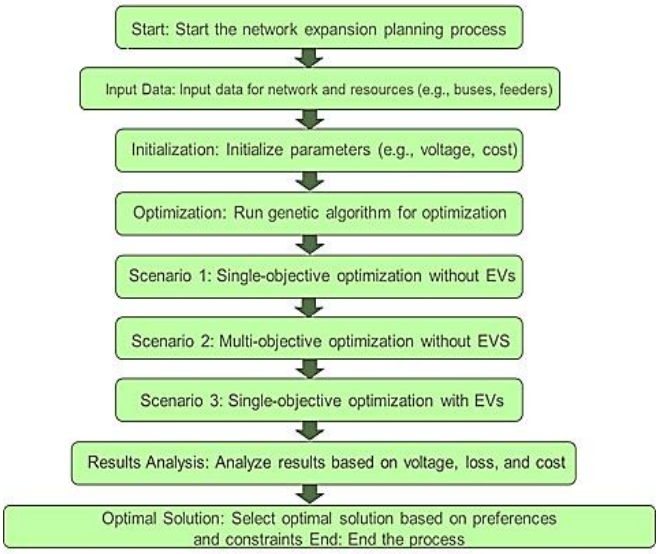

Fig. 1. Overall flowchart of the proposed solution method

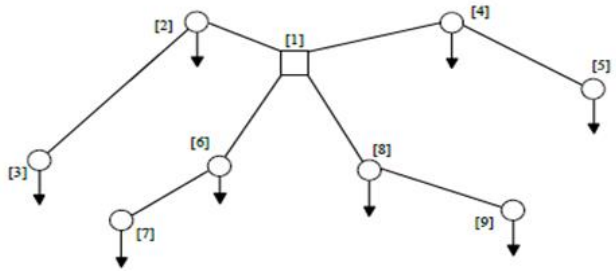

Fig. 2. Overall flowchart of the proposed Solution method

It is assumed that the battery capacity in the blocks is 10-megawatt amperes (for example, each transformer for increasing the capacity has a 10-megawatt ampere capacity), and the cost is $2 million. Also, the cost of purchasing power from the higher-level network (over the distribution network) for the high-voltage network is assumed to be $70 per megawatt-hour. For the distributed generation sources, it is assumed that they are of the wind and solar types, and the capital investment and operating costs for them are assumed to be $5 million per megawatt and $70 per megawatt-hour, respectively. Finally, the study horizon and the rate of return are assumed to be 4 years and 12.5%, respectively. In the third scenario, information related to electric vehicles will be provided and then the expansion of the network, considering this information, will be conducted.

4.1.1 Network with 9-bus

The topology of this network is shown in Fig. 2. The above-distributed bus-bar (32.133K Watt) is specified with number 1 in the diagram. The capacity of the existing bus-bar is 40 megawatts, and the growth rate target is 28% per year. The permissible voltage range is considered to be between 95% and 105%.

In this section, the study has been conducted in two forms. Initially, the study was carried out as a single-objective analysis, considering individual objectives, and then the study was extended to a multi-objective analysis. Additionally, in order to demonstrate the effect of considering the sources of generation of disturbances in the issue of distribution network expansion, each of the studies was conducted in two forms: with and without considering the sources of generation of disturbances.

4.1.1.1 Single Objective

The results of this study for both cases, with and without considering Distributed Generation (DG), are presented in Tables 1 and 2. Table 1 presents the values of the objective functions, and Table 2 presents the values of the decision variables of the problem (selection of equipment for expansion). It is worth mentioning that the total population in this study is 100, and the number of repetitions is also considered to be 100. The capacity of each generation source in this case is assumed to be 5 megawatts, with a purchase and installation cost of 5 million dollars. Also, the purchase and installation cost of each 10-megawatt bus-bar is assumed to be 10 million dollars. It should be noted that, in practice, the cost of developing a bus-bar is lower compared to the cost of the generation sources, but due to the fact that the study is conducted on the distribution network, the land cost is higher, and in the case of high land costs, gas-based backup units must be installed, with the construction cost being high as well. Another point is that the objective of the study without DG is purely based on costs, as if the generation source is not installed in the network, it will have no impact on losses or voltage.

4.1.1.2 Multi-Objective

By Pareto optimal solutions, we mean solutions where none of them is superior to the others in all objectives. For example, the Pareto

front of these solutions is shown in Table 3, where a careful examination of the objective function values reveals that none of the solutions is superior to the others in all objectives. This defines the set of Pareto optimal solutions. It should be noted that in this study, the number of Pareto set members is 1000, and the number of populations and repetitions is assumed to be the same as in the previous case. Fig. 3 illustrates the graphical representation of the Pareto front space of solutions

Table 1. Objective function values for network 9 based on the single objective solution

Objective function considered with DG			Without DG	
losses	Voltage deviation	Cost	Cost	
80	80	45	20	Expansion cost (M$)
0.2223	0.2223	0.30986	0.36986	Voltage deviation (%)
0.5987	0.5987	1.0011	1.5077	Losses (MW)

Table 2. Objective function values for network 9 based on the single objective solution

Objective function considered with DG												Without DG	
Loss				Voltage deviation				Cost					
DG	Location	Tr	Location	DG	Location	Tr	Location	DG	Location	Tr	Location	Post	Location
4	3	-	-	4	3	-	-	1	2	1	1	2	1
4	5	-	-	4	5	-	-	4	3	-	-		
4	7	-	-	4	7	-	-	1	5	-	-		
4	9	-	-	4	9	-	-	1	6	-	-		
-	-	-	-	-	-	-	-	2	9	-	-		

Table 3. Values of objective function variables and equipment for network 9 bus on multi-objective solution

	Answer 1	Answer 2	Answer 3	Answer 4	Answer 5	Answer 6
Expansion cost (M$)	55	60	65	80	80	80
Voltage deviation (%)	0.3059	0.2742	0.2652	0.2323	0.2342	0.2223
Losses (MW)	1.0011	0.8256	0.7716	0.6444	0.6357	0.5987
Post	1	0	0	0	0	0
Generator	9	12	13	16	16	16
Node number	Number of DGs					
2	1	1	1	1	1	0
3	4	4	4	4	4	4
4	0	0	0	0	0	0
5	1	2	2	4	3	4
6	0	0	0	0	0	0
7	1	2	2	3	4	4
8	0	0	0	0	0	0
9	2	3	3	4	4	4

4.1.2 Network with 30 Bus

The next set of studies involves the distribution network 30 with a bus-bar voltage of 11.63 kV, as shown in Fig. 3. The existing bus-bar capacity is 12 MVA, with a load demand of 10.244 MW and a forecast load in the year 13.291 MW. The capacity of the generation source ranges from 1.0 MW and a maximum feasible installation in each group is assumed to be 0.3 MW. The capacity of the expandable bus-bar is 10 MVA, and the allowable voltage range is between 90% and 110%. The scenario simulations for the wind and solar energy conditions are presented in Figs. 5 and 6. The probability associated with each scenario is provided in Table 4. In Figs. 5 and 6, the scenario quantities are based on the average capacity of the wind turbine and the solar photovoltaic cell. Each of the sources has an average capacity of 1 megawatt, with an installation and procurement cost of 2 million dollars considered. Additionally, the installation and procurement cost of each 4-megawatt wind farm is assumed to be 4 million dollars.

In the continuation of the study results, two primary case studies are included: one without electric vehicle charging and one where electric vehicle charging is considered. In the case where electric vehicles are not considered, the study mirrors the previous two scenarios: single-target and multi-target modes. For all studies in this section, a population of 150 and a repetition rate of 400 are assumed. In the multi-target study, the number of possible stored responses is assumed to be 1000.

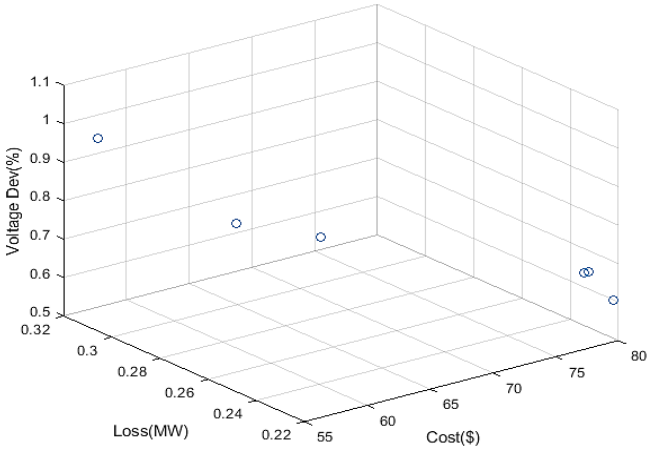

Fig. 3. Graphical representation of pareto front space for network 9 solutions.

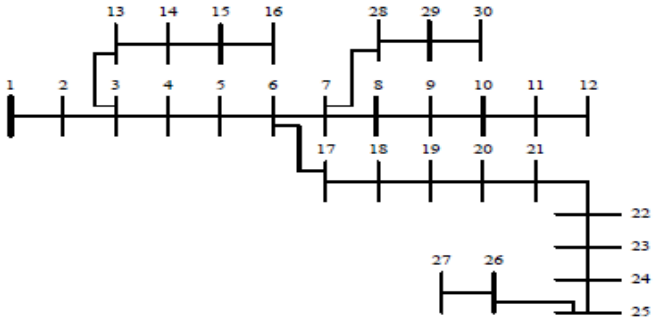

Fig. 4. Network with 30 Bus under study.

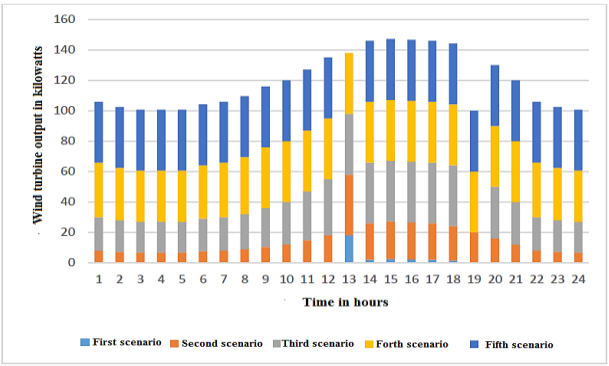

Fig. 5. Five different wind scenarios over a 24-hour period.

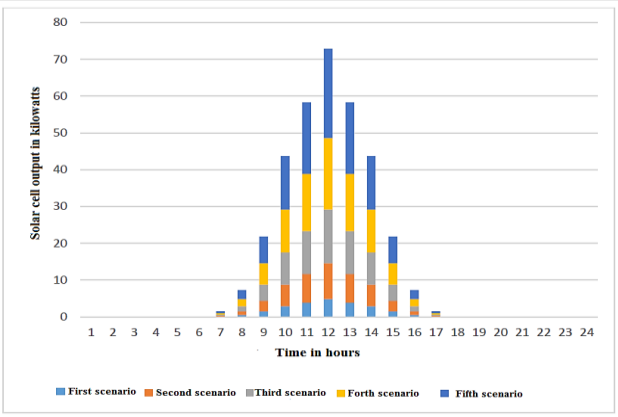

Fig. 6. Solar radiation scenarios over a 24-hour period.

Table 4. Probability of different wind and solar scenarios.

Scenario Number	Wind Scenario Probability	Solar Scenario Probability
1	0.18171	0.11809
2	0.37221	0.27875
3	0.28512	0.28398
4	0.12401	0.19262
5	0.03348	0.11971

Table 5. Objective function values for network 30 bus in single-objective solution.

Objective function considered with DG			Without DG	
losses	Voltage deviation	Cost	Cost	
16	16	8	4	Expansion cost (M$)
1.5466	1.5466	1.9279	2.8609	Voltage deviation (%)
0.5144	0.5144	0.5144	1.2689	Losses (MW)

Table 6. Values of independent variables (equipment selection) for network 30 bus in single-objective solution.

Objective function considered with DG												Without DG	
Loss				Voltage Deviation				Cost					
DG	Location	SS	Location	DG	Location	SS	Location	DG	Location	Tr	Location	Post	Location
2	8	-	-	2	3	-	-	1	19	1	1	1	1
3	9-12	-	-	3	9-12	-	-	3	20-27	-	-		
3	18-27	-	-	3	18-27	-	-	-	-	-	-		

4.1.2.1 Without Considering Electric Vehicles and Single-Objective

The results of this study are presented in Tables 5 and 6 for two cases, with and without considering the DG. In Table 5, the values of the objective function are shown, and in Table 4-6, the values of the variables of the problem (selection of equipment for expansion) are provided.

4.1.2.2 Without Considering Electric Vehicles in Multi-Objective

The Pareto front of these solutions is presented in Table 7. By carefully observing the objective function values, it is evident that none of the solutions is superior to the others in all objectives, which precisely defines the set of Pareto optimal solutions.

The graphical representation of the Pareto front space in this case is shown in Fig. 7. A notable point in this network is that there is no need for the expansion of the substation, and the entire additional load added to the network in the forecasted year is capable of being supplied by the installed generation sources. Therefore, it can be said that generation sources, in addition to their effect on losses and the voltage profile of the network, also delay the expansion of the substation. In fact, in this study, in the 4-year forecast, despite the presence of generation sources, there was no need to expand the substation.

Table 7. Objective Function Values and Selected Equipment for Expansion for Network 30 Bus in Multi-Objective Solution.

	Answer 1	Answer 2	Answer 3	Answer 4	Answer 5
Expansion cost (M$)	10	12	12	12	10
Voltage deviation (%)	1.5466	1.5854	1.7068	1.9058	1.9279
Losses (MW)	0.8043	0.78623	0.6259	0.53996	0.51444
Post	0	0	0	0	0
Generator	5	6	6	7	7

Table 8. Information on the number of electric vehicles at each bus station.

Bus Number	1	2	3	4	5	6	7	8	9
Number of vehicles	2	6	6	6	6	6	4	1	2
Bus Number	10	11	12	13	14	15	16	17	18
Number of vehicles	4	3	2	3	2	5	3	4	4
Bus Number	19	20	21	22	23	24	25	26	27
Number of vehicles	3	2	4	6	6	6	6	6	3

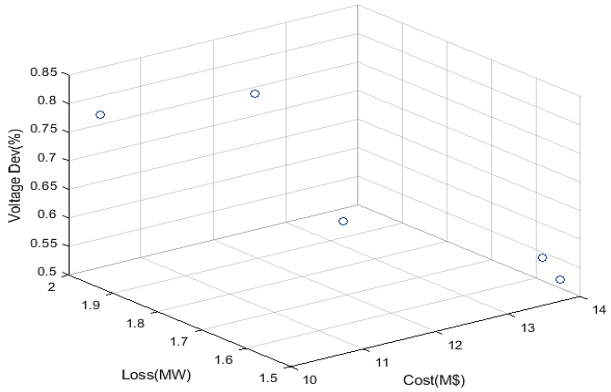

Fig. 7. Solar radiation scenarios over a 24-hour period.

4.2 Considering electric vehicles for multi-objective

In this section, the load of electric vehicles is added to the network, and the impact of the network expansion considering their load and the increased parking demand in the network is studied. Initially, the information of the electric vehicles is provided, and then the results of the study are broken down and analyzed.

The distribution data of electric vehicles is presented in Table 8, with their accessibility during the 24-hour period and their usage profile as detailed in the sequential table. Furthermore, Table 9 and Fig. 8 illustrate this information. The graphical representation of these responses is shown in Table 9. It should be noted that none of the responses in all objectives are superior to others, and this defines the set of typical answers

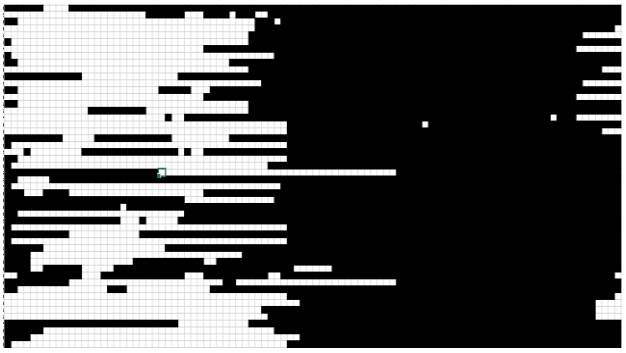

Fig. 8. Accessibility of vehicles over a 24-hour period.

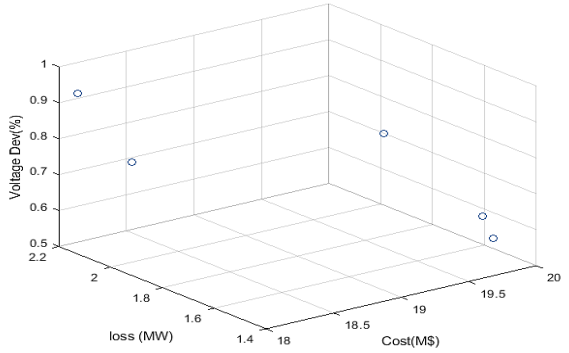

Fig. 9. Graphical representation of the Pareto front space for the 30-bus network, excluding electric vehicles

Table 9. Objective Function Values and Selected Equipment for Expansion for Network 30 Bus in Multi-Objective Solution.

	Answer 1	Answer 2	Answer 3	Answer 4	Answer 5
Expansion cost (M$)	18	18	20	20	20
Voltage deviation (%)	2.1261	1.9164	1.9878	1.6086	1.5658
Losses (MW)	0.9463	0.8153	0.6987	0.57865	0.52875
Post	1	0	1	0	0
Generator	7	9	8	10	10

The graphical representation of these responses is shown in Table 9. It should be noted that none of the responses in all objectives are superior to others, and this defines the set of typical answers. In this case, two parking spaces have been expanded in the network, one for buses 1 to 16 and 28 to 30, and the other for the remaining buses. The first parking space is installed at bus 10, and the second parking space is installed at bus 21. The location of the installation of the energy generation sources is similar to the previous case, but the additional amount of these sources compared to the previous study is installed at the parking locations. The parking space for the responses in this case corresponds to Fig.8.

5. Conclusion

In this paper, a genetic optimization algorithm was presented for solving the nonlinear problem of the expansion of backup distribution systems, considering the integration of energy generation sources. The goal of developing backup systems was to minimize costs, which, with the addition of energy generation sources, reduced deviations in voltage and losses. The problem also expanded to address the issue of increased generation losses. Ultimately, the proposed model was applied to a research system, and the results obtained from the study are as follows:

1. Selection in the Expanded Mode, the expansion program for the distribution network, combined with the expansion of energy generation sources, resulted in the expansion of two objective functions—voltage and transmission losses. The model, when moving towards the expansion of backup systems, showed that the transmission losses and voltage remained unchanged, but the costs of backup expansion decreased. On the other hand, as the problem moved toward further expansion of energy generation sources, transmission losses and voltage improved, but the expansion cost increased. Therefore, the solutions derived from this study will demonstrate these trends.

2. Use of Genetic Algorithms, Since the regular model was not capable of obtaining suitable answers, the genetic optimization algorithm was employed to solve this problem.

3. Provided Model's Capability, the proposed model was able to provide a space of optimal solutions that could help select the best solution based on engineering considerations. Additionally, in this paper, a ranking method was used for selecting the optimal solution.

4. In Multi-Objective Solutions, In the multi-objective problem, the solutions showed a tendency to select more energy generation sources (see Table 4-2 results), because the presence of energy generation sources in the network helped reduce transmission losses.

5. In Multi-Objective Solutions, due to the significant improvement in transmission losses and voltage profile, the optimal solutions tend to favor the expansion of energy generation sources. Consequently, the solutions typically lean towards the expansion of energy sources rather than the expansion of backup systems.

6. Based on the results, it can be concluded that, the expansion of energy generation sources leads to a considerable delay in the expansion of backup systems. As an alternative, while offering much better technical outcomes, it might be preferable to consider replacing the expansion of backup systems with this method. However, to ensure there is no need for further backup system expansion, the issue should be addressed using a similar approach as in the current paper, particularly for network optimization.

7. With the increasing load of electric vehicles on the network, due to the increased load at parking points, energy generation sources have been added alongside this increased load. Thus, transmission losses and the voltage profile, despite the higher load from large parking stations, have not undergone significant changes.

References

[1] L. Blank and A. Tarquin, Engineering Economy. New York, NY, USA: McGraw-Hill, 2012.

[2] P.C. Paiva, H.M. Khodr, J.A. Domínguez-Navarro, J.M. Yusta, and A.J. Urdaneta, “Integral planning of primary-secondary distribution systems using mixed integer linear programming,” IEEE Trans. Power Syst., vol. 20, no. 2, pp. 1134–1143, May 2015.

[3] S. Ganguly, N.C. Sahoo, and D. Das, “Recent advances on power distribution system planning: a state-of-the-art survey,” Energy Syst., vol. 4, no. 2, pp. 165–193, Jun. 2018.

[4] C.L.T. Borges and V.F. Martins, “Multistage expansion planning for active distribution networks under demand and distributed generation uncertainties,” Int. J. Electr. Power Energy Syst., vol. 36, no. 1, pp. 107– 116, Mar. 2019.

[5] M.E. Samper and A. Vargas, “Investment decisions in distribution networks under uncertainty with distributed generation—Part I: Model formulation,” IEEE Trans. Power Syst., vol. 28, no. 3, pp. 2331–2340, Aug. 2018.

[6] G. Muñoz-Delgado, J. Contreras and J.M. Arroyo, “Multistage generation and network expansion planning in distribution systems considering uncertainty and reliability”, IEEE Trans. Power Syst., vol. 31, no. 5, pp. 3715–3728, Sep. 2016.

[7] M. Asensio, P. Meneses de Quevedo, G. Muñoz-Delgado and J.

Contreras, “Joint distribution network and renewable energy expansion planning considering demand response and energy storage—Part I: Stochastic programming model,” IEEE Trans. Smart Grids, in press. [Online]. Available http :// ieeexplore.ieee.org/ stamp/ stamp.jsp? arnumber=7462292

[8] S. Wogrin, D. Galbally and J. Reneses, “Optimizing storage operations in medium-and long-term power system models,” IEEE Trans. Power Syst., vol. 31, pp. 3129–3138, Jul. 2016.

[9] M. Sedghi, A. Ahmadian and M. Aliakbar, “Optimal storage planning in active distribution network considering uncertainty of wind power distributed generation,” IEEE Trans. Power Syst., vol. 31, pp. 304-316, Jan. 2019.

[10] X. Shen, M. Shahidehpour, Y. Han, S. Zhu and J. Zheng, "Expansion Planning of Active Distribution Networks with Centralized and Distributed Energy Storage Systems," IEEE Transactions on Sustainable Energy, vol. 8, no. 1, pp. 126-134, Jan. 2017.

[11] H. Akhavan and H. Mohsenian, “Energy storage planning in active distribution grids: A chance-constrained optimization with non-parametric probability functions,” IEEE Trans. Smart Grids, in press. [Online]. Available: ttp :// ieeexplore.ieee.org / stamp / stamp.jsp ? arnumber=7556322.

[12] A. Ahmadian, M. Sedghi and M. Aliakbar-Golkar, "Fuzzy Load Modeling of Plug-in Electric Vehicles for Optimal Storage and DG Planning in Active Distribution Network," IEEE Transactions on Vehicular Technology, vol. 66, no. 5, pp. 3622-3631, May 2017.

[13] Z. Liu, F. Wen and G. Ledwich, “Optimal planning of EVCS in distribution systems,” IEEE Trans. Power Deliv., vol. 28, pp. 102–110, no. 1, Jan. 2019.

[14] B. Liu, X. Huang, J. Li, X. Qian and J. Cheng, “Multi-objective planning of distribution network containing distributed generation and electric vehicle charging stations,” Dianwang Jishu/Power System Technology, vol. 39, no. 2, pp. 450–456, Oct. 2020.

[15] W. Yao, J. Zhao, F. Wen, Z. Dong, Y. Xue, Y. Xu and K. Meng, “A multiobjective collaborative planning strategy for integrated power distribution and electric vehicle charging systems,” IEEE Trans. Power Syst., vol. 29, no. 4, pp. 1811–1821, Jul. 2018.

[16] Y. Weifeng, C.Y. Chung, W. Fushuan, Q. Mingwen and X. Yusheng, “Scenario-based comprehensive expansion planning for distribution systems considering integration of plug-in electric vehicles,” IEEE Trans.Power Syst., vol. 31, no. 1, pp. 317–328, Jan. 2016.

[17] Zare, Peyman, Abdolmajid Dejamkhooy, and Iraj Faraji Davoudkhani. "Efficient expansion planning of modern multi-energy distribution networks with electric vehicle charging stations: A stochastic MILP model." *Sustainable Energy, Grids and Networks* 38 (2024): 101225.

[18] Singh, Bindeshwar, and Pankaj Kumar Dubey. "Distributed power generation planning for distribution networks using electric vehicles: Systematic attention to challenges and opportunities." *Journal of Energy Storage* 48 (2022): 104030.

[19] Zhou, Siyu, Yang Han, Karar Mahmoud, Mohamed MF Darwish, Matti Lehtonen, Ping Yang, and Amr S. Zalhaf. "A novel unified planning model for distributed generation and electric vehicle charging station considering multi-uncertainties and battery degradation." *Applied Energy* 348 (2023): 121566.

[20] Yuvaraj, Thangaraj, Thirukoilur Dhandapani Suresh, Arokiasamy Ananthi Christy, Thanikanti Sudhakar Babu, and Benedetto Nastasi. "Modelling and allocation of hydrogen-fuel-cell-based distributed generation to mitigate electric vehicle charging station impact and reliability analysis on electrical distribution systems." *Energies* 16, no. 19 (2023): 6869.

[21] Yuvaraj, T., K. R. Devabalaji, J. Anish Kumar, Sudhakar Babu Thanikanti, and Nnamdi I. Nwulu. "A comprehensive review and analysis of the allocation of electric vehicle charging stations in distribution networks." *IEEE Access* 12 (2024): 5404-5461.

[22] Rene, Ebunle Akupan, Willy Stephen Tounsi Fokui, and Paule Kevin Nembou Kouonchie. "Optimal allocation of plug-in electric vehicle charging stations in the distribution network with distributed generation." Green Energy and Intelligent Transportation 2, no. 3 (2023): 100094.

[23] Da Silva, Enielma Cunha, Ozy D. Melgar-Dominguez, and Rubén Romero. "Simultaneous distributed generation and electric vehicles hosting capacity assessment in electric distribution systems." *IEEE Access* 9 (2021): 110927-110939.

[24] Eid, Ahmad, Osama Mohammed, and Hassan El-Kishky. "Efficient operation of battery energy storage systems, electric-vehicle charging stations and renewable energy sources linked to distribution systems." *Journal of Energy Storage* 55 (2022): 105644.

[25] Li, Ke, Chengcheng Shao, Zechun Hu, and Mohammad Shahidehpour. "An MILP method for optimal planning of electric vehicle charging stations in coordinated urban power and transportation networks." *IEEE Transactions on Power Systems* 38, no. 6 (2022): 5406-5419.

[26] Aljafari, Belqasem, T. Yuvaraj, R. Hemalatha, Sudhakar Babu Thanikanti, and Nnamdi Nwulu. "Optimizing radial distribution system with distributed generation and EV charging: a spotted hyena approach." *IEEE Access* (2024).

[27] Yaghoubi-Nia, Mohammad-Reza, Hamed Hashemi-Dezaki, and Abolfazl Halvaei Niasar. "Optimized allocation of microgrids’ distributed generations and electric vehicle charging stations considering system uncertainties by clustering algorithms." *IET Renewable Power Generation* 18, no. 11 (2024): 1798-1818.